Molecular Crystals and Liquid Crystals
Publication details, including instructions for authors and subscription information:
http://www.tandfonline.com/loi/gmcl16

Meltingk Behaviour of Ideal Ascending Solid Solutions

George W. Smith [a]
[a] Physics Department General Motors Research Laboratories Warren, Michigan, 48090.
Version of record first published: 20 Apr 2011.

To cite this article: George W. Smith (1981): Meltingk Behaviour of Ideal Ascending Solid Solutions, Molecular Crystals and Liquid Crystals, 65:3-4, 285-306

To link to this article: http://dx.doi.org/10.1080/00268948108082139

Mol. Cryst. Liq. Cryst., 1981, Vol. 65, pp. 285–306
0026-8941/81/6504–0285$06.50/0

Melting Behavior of Ideal Ascending Solid Solutions

GEORGE W. SMITH

Physics Department, General Motors Research Laboratories, Warren, Michigan 48090.

(*Received April 10, 1980*)

An expression for the melting curve of an ideal binary ascending solid solution has been derived and tested by comparison with experimental melting curves for three systems. Agreement with experiment is better for two organic binaries (bromobenzene/chlorobenzene and 1.12-benzoperylene-coronene) than for a metal (bismuth/antimony). A theoretical expression for the curvature of liquidus and solidus lines for a binary of components having small latent heats has been derived. The curvature is determined solely by the relative magnitudes of the latent heats and melting temperatures of the components.

I INTRODUCTION

Although several types of phase diagrams for solid binary solutions are known,[1–3] the details of the melting behavior of even the simplest of these systems have evidently not been closely examined theoretically. We have previously calculated the melting behavior of a binary eutectic-forming system.[4] The calculation gave satisfactory agreement with melting curves determined by differential scanning calorimetry (DSC). In the present report, we examine the simplest of the binary solid solutions: Type I of Hildebrand and Scott[1] and Findlay[3] (also designated the ascending solid solution).[2] For a special case of Type I, the *ideal* ascending solid solution, we shall calculate DSC melting behavior for comparison with experiments on three binary systems, one of them a mixture of two planar aromatics.

II BASIC ASSUMPTIONS

The assumptions basic to a derivation of the solidus and liquidus curves for an ideal binary ascending solid solution are three in number:[1–3]

1) The two components of the binary system crystallize in an ideal disordered solid solution over the entire composition range. That is, the interaction potential between component molecules is composition-independent and the heat of mixing is zero. Furthermore, the components do not react chemically, form compounds, or undergo an order-disorder transformation.

2) The binary liquid phase is likewise an ideal solution.

3) The enthalpies of melting (latent heats) of the pure components are independent of temperature. (This is equivalent to the assumption that the difference of the heat capacities of the solid and liquid phases of the pure components is zero).[5]

The equations of the liquidus or solidus lines have been derived[1–3] on the basis of these assumptions and are given in Eqs. (1) and (2). Figure 1 illustrates the phase diagram schematically. (From the figure the reason for the term "ascending solid solution" is made clear: this simplest solid solution system exhibits melting point variation that is monotonic with composition, lying between the melting points of the end members.)

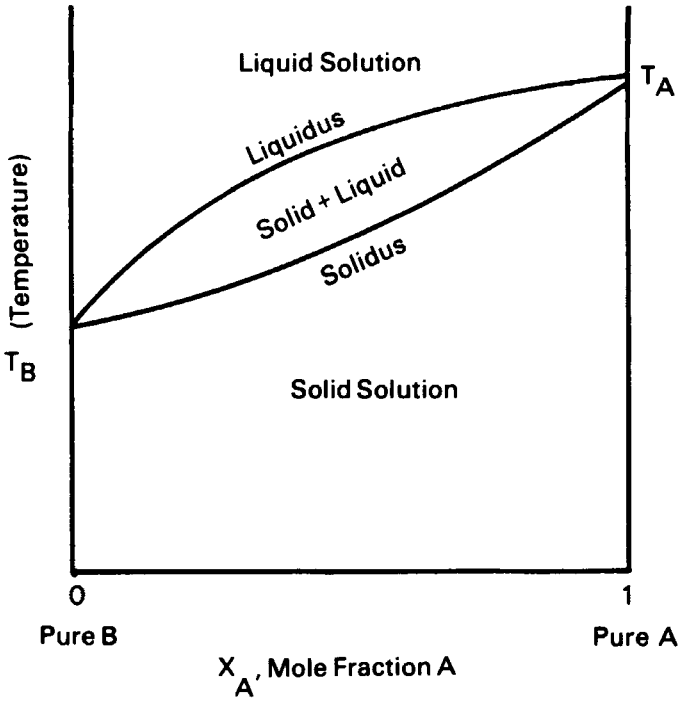

FIGURE 1 Schematic phase behavior for an ideal ascending solid solution.

Liquidus:

$$X_A^l = \frac{1 - e^{\lambda_B}}{e^{\lambda_A} - e^{\lambda_B}} \tag{1}$$

Solidus:

$$X_A^S = \frac{1 - e^{\lambda_B}}{1 - e^{\lambda_B - \lambda_A}} = e^{\lambda_A} X_A^l \tag{2}$$

where:

X_A^l, X_A^S are the mole fractions of component A on the liquidus and solidus curves, respectively.

$$\lambda_A = \frac{L_A}{R}\left(\frac{1}{T} - \frac{1}{T_A}\right) \tag{3}$$

$$\lambda_B = \frac{L_B}{R}\left(\frac{1}{T} - \frac{1}{T_B}\right) \tag{4}$$

L_A, L_B are the latent heats of melting of pure A and pure B, respectively; R is the gas constant; T the absolute temperature; and T_A, T_B the melting temperatures of A and B.

In order to derive the DSC melting curves, it will be necessary to know n_A^{sol} and n_B^{sol}, the number of moles of solid A and solid B, as a function of temperature and composition in the mixed phase region (i.e., between the liquidus and solidus curves). To help us to visualize the derivation of these quantities, we redraw the schematic diagram of Figure 1 in the form seen in Figure 2. The mixed-phase region (between liquidus and solidus) consists of a mixture of liquid, having mole fraction X_A^l, and solid, having mole fraction X_A^S. The ratio of the total number of moles of liquid, n_{liq}, to the total number of moles of solid, n_{sol}, at temperature T and total concentration X_A is given by the lever rule:[6,7]

$$\frac{n_{\text{liq}}}{n_{\text{sol}}} = \frac{X_A^S - X_A}{X_A - X_A^l}. \tag{5}$$

It is easy to rewrite this equation to find n_{sol} in terms of n, the total number of moles of A and B in the mixture ($n = n_A + n_B = n_{\text{liq}} + n_{\text{sol}}$). Thus,

$$n_{\text{sol}} = \frac{X_A - X_A^l}{X_A^S - X_A^l} n. \tag{6}$$

Since

$$n_A^{\text{sol}} \equiv X_A^S n_{\text{sol}} \tag{7}$$

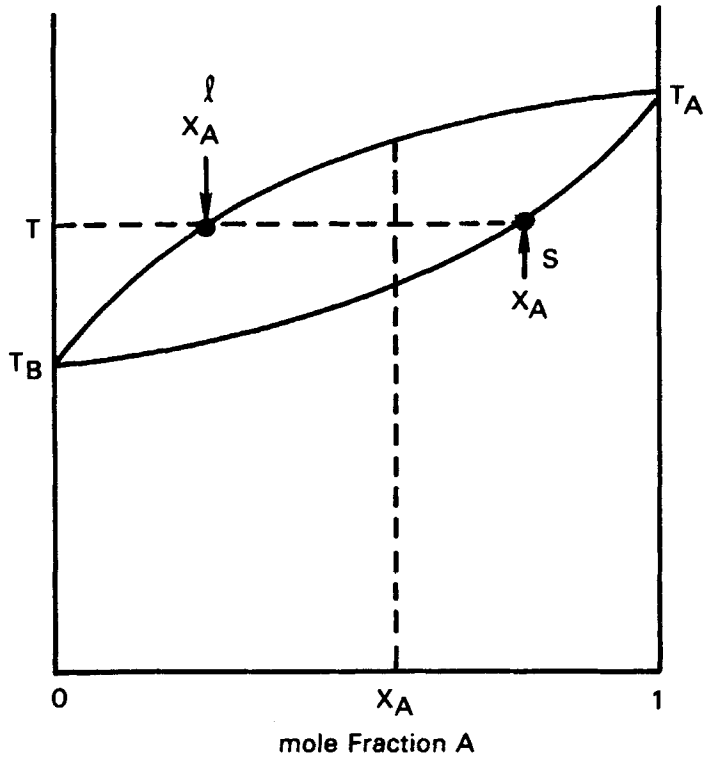

FIGURE 2 Schematic phase diagram of ascending solid solution.

and

$$n_B^{\text{sol}} \equiv X_B^S n_{\text{sol}} = (1 - X_A^S) n_{\text{sol}} = \left(\frac{1 - X_A^S}{X_A^S}\right) n_A^{\text{sol}}, \tag{8}$$

we have

$$n_A^{\text{sol}} = \frac{X_A^S (X_A - X_A^l) n}{(X_A^S - X_A^l)} \tag{9}$$

$$n_B^{\text{sol}} = (1 - X_A^S)\left(\frac{X_A - X_A^l}{X_A^S - X_A^l}\right) n \tag{10}$$

or, from Eq. (2),

$$n_A^{\text{sol}} = e^{\lambda_A}\left(\frac{X_A - X_A^l}{e^{\lambda_A} - 1}\right) n = \left(\frac{X_A - X_A^l}{1 - e^{-\lambda_A}}\right) n \tag{11}$$

$$n_B^{sol} = (1 - e^{\lambda_A} X_A^l)\left(\frac{X_A - X_A^l}{e^{\lambda_A} X_A^l - X_A^l}\right) n = \frac{(e^{-\lambda_A}/X_A^l - 1)(X_A - X_A^l)}{(1 - e^{-\lambda_A})} n \quad (12)$$

It is now necessary to make a fundamental simplification concerning the amount of absorbed heat needed to melt an increment of the solid solution. We shall assume that the same heat quantity ΔQ_A is required to melt Δn_A moles of A whether A is in solid solution or in pure A (and similarly for B). Although this assumption seems drastic, there is a certain amount of reasonableness to it. Indeed, the similarities of molecular structures, lattices, and intermolecular interactions of A and B required to yield a solid solution in the first place[2] (see basic assumption 1 above), seem to be consistent with this simplification. It has the added advantage that it renders tractable the algebra which follows.

On the basis of the simplifying assumption, we write the following expression for the amount of heat ΔQ absorbed in melting an increment of the solid solution:

$$\Delta Q = -(\Delta n_A^{sol} L_A + \Delta n_B^{sol} L_B). \quad (13)$$

The minus sign is present in order to yield a positive latent heat increment for a decrease in n_A^{sol} or n_B^{sol}. The quantity dQ/dT (proportional to DSC signal strength)[4] is thus:

$$\frac{dQ}{dT} = -\left(L_A \frac{dn_A^{sol}}{dT} + L_B \frac{dn_B^{sol}}{dT}\right) \quad (14)$$

The total quantity of heat to melt the entire solid solution sample is then:

$$Q = n_A L_A + n_B L_B \quad (15)$$

which on a molar basis is

$$L = \frac{Q}{n} = X_A L_A + X_B L_B = X_A L_A + (1 - X_A) L_B \quad (16)$$

In the next section we shall derive an expression for dQ/dT as a function of T and X_A.

III CALCULATION OF DSC MELTING CURVE

From Eq. (14), it is apparent that expressions for dn_A^{sol}/dT and dn_B^{sol}/dT are needed in order to calculate dQ/dT. However, we shall rewrite Eq. (14)

entirely in terms of n_A^{sol} and X_A^S

$$\frac{dQ}{dT} = -\left(L_A\frac{dn_A^{sol}}{dT} + L_B\frac{dn_B^{sol}}{dT}\right) = -\left[L_A\frac{dn_A^{sol}}{dT} + L_B\frac{d}{dT}\left\{\left(\frac{1}{X_A^S} - 1\right)n_A^{sol}\right\}\right]$$

$$= -\left[(L_A - L_B)\frac{dn_A^{sol}}{dT} + \frac{L_B}{X_A^S}\frac{dn_A^{sol}}{dT} - \left(\frac{1}{X_A^S}\right)^2 n_A^{sol}L_B\frac{dX_A^S}{dT}\right] \tag{17}$$

Differentiation of Eq (2) and some algebraic manipulation yields

$$\frac{dX_A^s}{dT} = \frac{e^{\lambda_A+\lambda_B}[L_A(1 - e^{\lambda_B} - L_B(1 - e^{\lambda_A})]}{[e^{\lambda_A} - e^{\lambda_B}]^2RT^2} \tag{18}$$

A similar mathematical treatment based on Eq. (9) yields:

$$\frac{dn_A^{sol}}{dT} = \frac{ne^{\lambda_A}}{(1 - e^{\lambda_A})^2RT^2}$$

$$\times\left[X_AL_A + \frac{L_A(1 - e^{\lambda_B})(e^{\lambda_B} - e^{2\lambda_A}) - L_Be^{\lambda_B}(1 - e^{\lambda_A})^2}{(e^{\lambda_A} - e^{\lambda_B})^2}\right] \tag{19}$$

Substitution of Eqs. (18) and (19) into Eq. (17), followed by a more extended algebraic struggle, leads to the desired expression for dQ/dT:

$$\frac{dQ}{dT} = Q_1 + Q_2 + Q_3 + Q_4 \qquad (\text{for } X_A^l < X_A < X_A^S) \tag{20}$$

$$= 0 \qquad (\text{for } X_A < X_A^l;\ X_A > X_A^S)$$

where

$$Q_1 = \left(\frac{-nX_A}{RT^2}\right)\left[\frac{L_A^2e^{\lambda_A}}{(1 - e^{\lambda_A})^2} - \frac{L_B^2e^{\lambda_B}}{(1 - e^{\lambda_B})^2}\right] \tag{21}$$

$$Q_2 = \frac{2nL_AL_Be^{\lambda_A+\lambda_B}}{RT^2(e^{\lambda_A} - e^{\lambda_B})^2} \tag{22}$$

$$Q_3 = \left(\frac{-nL_B^2}{RT^2}\right)\frac{e^{\lambda_A+\lambda_B}}{(e^{\lambda_A} - e^{\lambda_B})^2} \tag{23}$$

$$Q_4 = \left(\frac{-nL_A^2}{RT^2}\right)\left[\frac{e^{\lambda_A+\lambda_B}}{(e^{\lambda_A} - e^{\lambda_B})^2}\right]\frac{(1 - e^{\lambda_B})(1 - e^{2\lambda_A-\lambda_B})}{(1 - e^{\lambda_A})^2} \tag{24}$$

The correctness of Eq. (20) can be tested by a simple symmetry check. Substitution of $(1 - X_B)$ for X_A in Eq. (21) and subsequent rearrangement of terms in Eq. (20) should yield an expression analogous to Eq. (20):

$$\frac{dQ}{dT} = Q_1' + Q_2' + Q_3' + Q_4' \tag{25}$$

in which all A and B subscripts are interchanged. It can be easily verified that Eq. (20) does indeed pass the symmetry test. A more rigorous test, comparison with experiment, is examined in Section V below.

IV REMARK ON EXPERIMENTAL PROCEDURE

All DSC measurements on binary systems reported here were performed on samples "mixed *in situ*," a technique developed recently in this laboratory for use with rare and/or hazardous specimens. Because only a few milligrams of material are available in the case of some of our samples, it is essential to use as little material as possible for each experiment. (The procedure is useful also in minimizing the likelihood of spillage of hazardous species.)

In the *in-situ* method, all components of a mixture are weighed individually into an aluminum DSC pan to which an aluminum lid is then hermetically sealed by means of a Perkin–Elmer standard cold-welding tool. These procedures all take place in an enclosure to minimize the influence of drafts or possible dangers of spillage. The sealed mixture is then placed in a small vial for transport to the DSC instrument.

Once the sample is placed in the calorimeter, its temperature is scanned through the presumed range of interest, while the DSC spectrum is simultaneously recorded. After several such cycles, the spectrum becomes more-or-less reproducible, indicating a steady state. The method has been tested on liquid crystal binaries previously studied in our laboratory and does seem to yield adequately mixed systems.

The calorimeter used in the present studies is a Perkin–Elmer DSC-2 which has recently been equipped with a Perkin–Elmer Programmable Calculator System C for rapid processing of data. The instrument was calibrated using an indium standard ($L_m = 28.41$ kJ/kg).

The data cited in this report were obtained using the DSC/computer combination with the exception of those for the planar aromatics, which were studied prior to the acquisition of the system.

Finally, in the case of materials with the lowest melting temperatures (Cl ϕ and Br ϕ/Cl ϕ with high Cl ϕ concentrations), it was necessary to quench the sample in liquid nitrogen immediately before transfer (at low temperature) to the DSC in order to obtain crystallization.

V COMPARISON WITH EXPERIMENT

Relatively few systems are known to form ideal solid solutions.[1] It may be that the degree to which DSC melting curves agree with those calculated from Eq. (20) will complement temperature-composition plots as a test of

ideality. In order to compare theory to experiment, we have written a BASIC computer program to calculate liquidus and solidus (Eqs. (1) and (2)) and the DSC melting curve (Eq. 20)). This program, SLHEAT, is listed in Table I. The results of the melting curve calculation are also accessible to a plotting routine.[8] Three binaries were investigated in order to test Eqs. (1), (2), and (20). Two of these systems, have been studied previously: bromobenzene/chlorobenzene[1] and bismuth/antimony[1,9] constitute ascending solid solutions (Type I) over their entire composition range.

TABLE I

Listing of SLHEAT

```
SLHEAT    16 AUG 79  16:44

90 FILE#1: "PLOTDATA"
100 PRINT "FOR COMP 1, WHAT ARE NAME, T1(K), H1(CAL/MOL)"
110 INPUT A$,T1,H1
120 PRINT "FOR COMP 2, WHAT ARE NAME,T2(K),H2(CAL/MOL)"
130 INPUT B$,T2,H2
135 PRINT "SOLIDUS, LIQUIDUS MOL FRACS FOR COMP 1 (IDEAL SOLID SOLUTION)"
140 PRINT "TEMP (K)", "SOLIDUS COMP", "LIQUIDUS COMP"
150 FOR T = T2 TO T1 STEP (T1 - T2)/20
160 IF T = T2 THEN 250
170 IF T = T1 THEN 270
190 LET L1 = (H1/1.987)*(1/T - 1/T1)
200 LET L2 = (H2/1.987)*(1/T - 1/T2)
210 LET L = (1 - EXP(L2))/(EXP(L1) - EXP(L2))
220 LET S = EXP(L1)*L
230 PRINT T,S,L
240 GO TO 350
250 PRINT T2,0,0
260 GO TO 350
270 PRINT T1,1,1
350 NEXT T
360 PRINT "DO YOU WANT DO/DT (1 = YES)";
370 INPUT U9
380 IF U9 <> 1 THEN 1000
390 PRINT "WHAT ARE TMIN (K), TMAX (K), AND X1";
400 INPUT T8,T9,X1
405 PRINT "TEMP(K)","01", "I*02", "I*03", "I*04", "I*01 + 02 + 03 + 04"
406 !CPATCH#1
410 FOR T = T8 TO T9 STEP (T9 - T8)/20
420 LET L1 = (H1/1.987)*(1/T - 1/T1)
430 LET L2 = (H2/1.987)*(1/T - 1/T2)
440 LET R1 = EXP(L1+L2)/((EXP(L1)-EXP(L2))^2*T^2)
450 LET 01 = (-X1/T)*((H1^2*EXP(L1))/((1-EXP(L1))^2))
460 LET 01 = 01 + (X1/T)*((H2^2*EXP(L2))/((1-EXP(L2))^2))
465 LET 01 = 01/T
470 LET 02 = 2*H1*H2*R1
480 LET 03 = -(H2^2)*R1
490 LET 04 = (-H1^2)*R1*(1-EXP(L2))*(1-EXP(2*L1-L2))/(1-EXP(L1))^2
500 PRINT T,01;02;03;04;01+02+03+04
505 PRINT#1: T;01;02;03;04;01+02+03+04
510 NEXT T
520 PRINT "DO YOU WANT TO RERUN DO/DT (1 = YES)";
530 INPUT U8
540 IF U8 <> 1 THEN 1000
550 PRINT "WHAT ARE NEW TMIN (K), TMAX (K), X1";
560 INPUT T8, T9, X1
570 GO TO 405
1000 END
```

A Chlorobenzene/bromobenzene

Of the group VII-substituted phenyls only bromobenzene/chlorobenzene exhibits a simple type I phase diagram.[1] However, the system is a difficult one with which to test the equations for an ideal solid solution. The fact that both components are liquids at room temperature makes for ease of mixing, but sample loss by vaporization during weighing makes accurate measurement of mass difficult. Nevertheless, accuracy adequate for our purposes was achievable. A greater concern was the narrowness of the mixed-phase regime, due to the similarity in magnitude of both latent heats and melting temperatures of the two components. As a result, it was not possible to resolve the liquidus and solidus lines.

In Table II are listed melting parameters for five members of the Br ϕ/Cl ϕ (ϕ = benzene) system. The width of the DSC line (due to impurities) for pure Br ϕ and Cl ϕ is ~ 3 K which, as we shall see, is large compared to the breadth of the mixed-phase region.

TABLE II

Melting Parameters for Br ϕ/Cl ϕ mixtures

$X_{Br\phi}$	T_i(K)[b]	T_f(K)[c]	T_m(K)[d]	L_m(kJ/mol)[e]	L_m(kJ/mol)[f]
0	228	231	228.1[g]	9.79	9.65[g]
0.230	229	234		10.18	
0.415	231	235.5		9.97	
0.538	232.7	236		9.90	
1.0	242	245	242.6[g]	10.23	10.64[g]

[a] $X_{Br\phi}$ = mole fraction Br ϕ.
[b] T_i = initial temperature of DSC transition, determined by extrapolation of peak leading edge to baseline.
[c] T_f = final temperature of DSC transition, similarly determined.
[d] T_m = melting temperature (from literature).
[e] Latent heat of melting (present work).
[f] Latent heat of melting (from literature).
[g] J. Timmermans, *Physical-Chemical Constants of Pure Organic Compounds*, Elsevier, N.Y. (1950).

In Figure 3, the liquidus and solidus calculated from Eqs. (1) and (2) are compared with experiment. It is clear that the breadth of the experimental transitions masks any attempt to resolve the liquidus and solidus. However, within experimental error the calculated and experimental temperatures are consistent, as are the calculated and experimental latent heats (Figure 4).

The calculated and experimental DSC melting curves for $X_{Br\phi} = 0.415$ are compared in Figures 5a and 5b. The differences between the two curves are ascribable to two factors: (1) the well-known tendency of the DSC

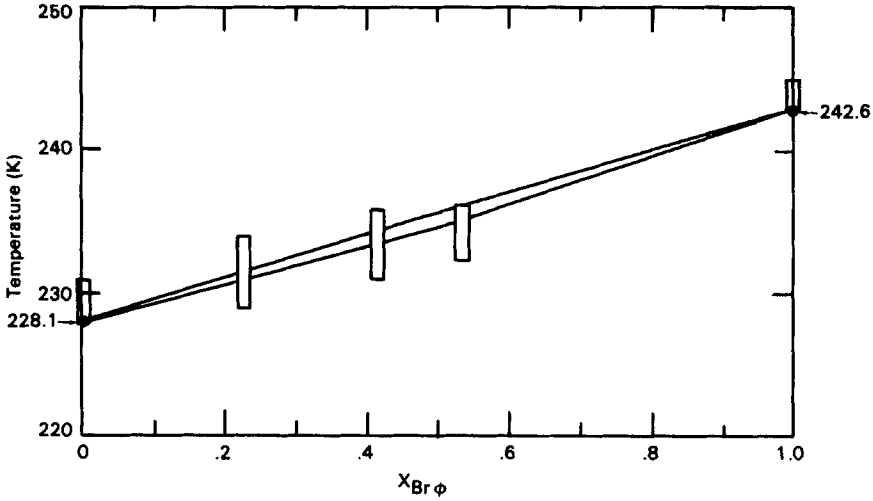

FIGURE 3 Phase diagram of Br ϕ/Clϕ. Solid lines = calculated liquidus and solidus. Bars = present experiment; circles = literature data.

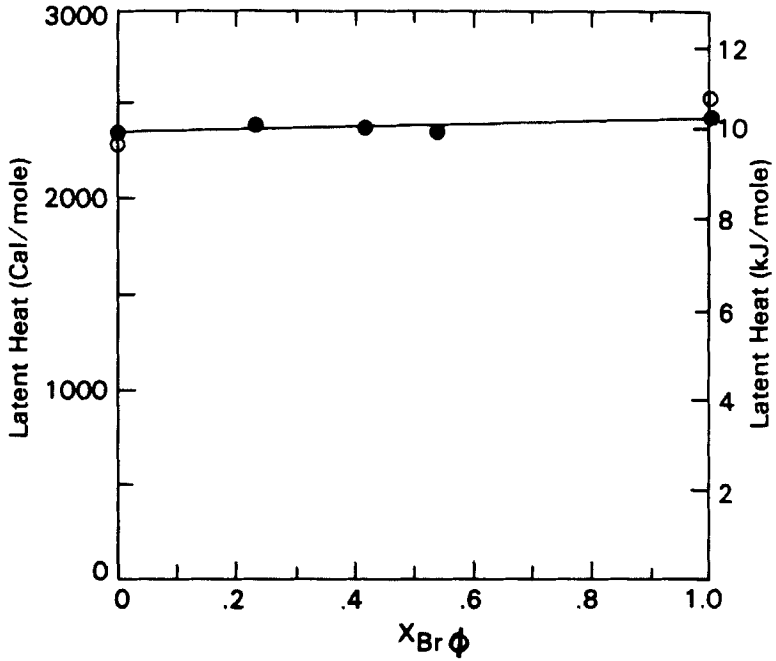

FIGURE 4 Latent heats for Br ϕ/Cl ϕ mixtures. Filled circles = present work; open circles = literature data.

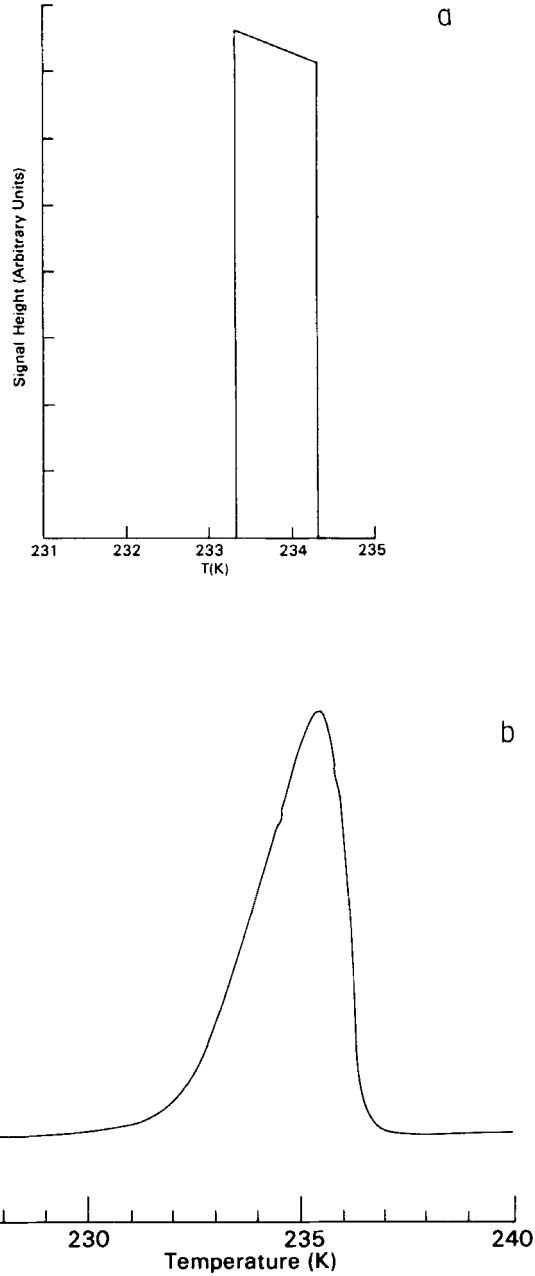

FIGURE 5(a) Calculated DSC melting curve for $X_{Br\phi} = 0.415$. (b) Experimental DSC melting curve for $X_{Br\phi} = 0.415$.

instrument to "smooth" sharp peaks[4] and (2) the broadening influence of impurities. The system Br ϕ/Cl ϕ, although agreeing with calculations, does not allow a clear-cut test of the theory. Therefore, we turn our attention to a second system, Bi/Sb.

B Bismuth/antimony

The phase diagram of the Bi/Sb system has been previously reported.[9] Because of difficulties of sample preparation,[10] the elevated temperatures required for samples with high Sb-content, and limitations of time, we studied only one binary mixture of Bi/Sb (for mole fraction $X_{Bi} = 0.834$). It was felt that this one mixture yielded a reasonable test of ideality (or lack of it) of the Bi/Sb system.[11] The thermal data for this sample plus that for pure Bi and pure Sb are summarized in Table III. The initial and final melting temperatures, T_i and T_f, for the binary sample were determined from the DSC melting curve of Figure 6.

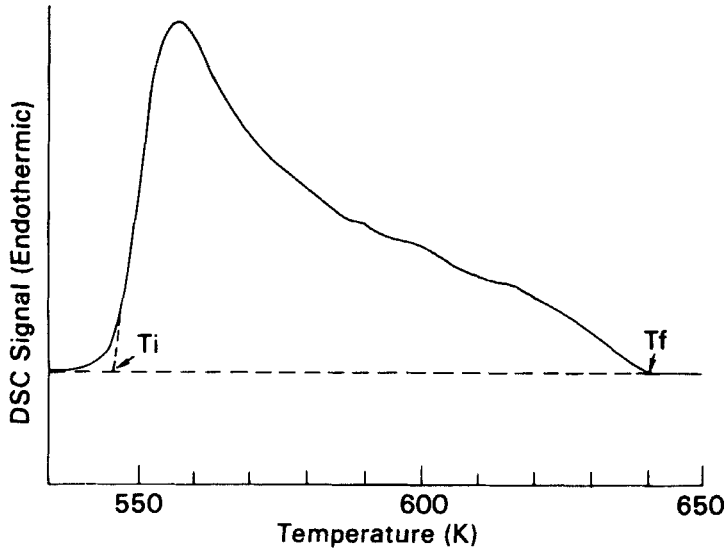

FIGURE 6 DSC melting curve for Bi/Sb sample with $X_{Bi} = 0.834$. Temperature scan rate 20°C/min; sample mass 22.73 mg.

In Figure 7 we compare the phase diagram of Bi/Sb calculated from Eqs. (1) and (2) (using the data of Table III) with the experimental ASM diagram.[9,12] Also plotted are the temperature extrema of the DSC melting curve of Figure 6. It is clear that the Bi/Sb is not an ideal solid solution.

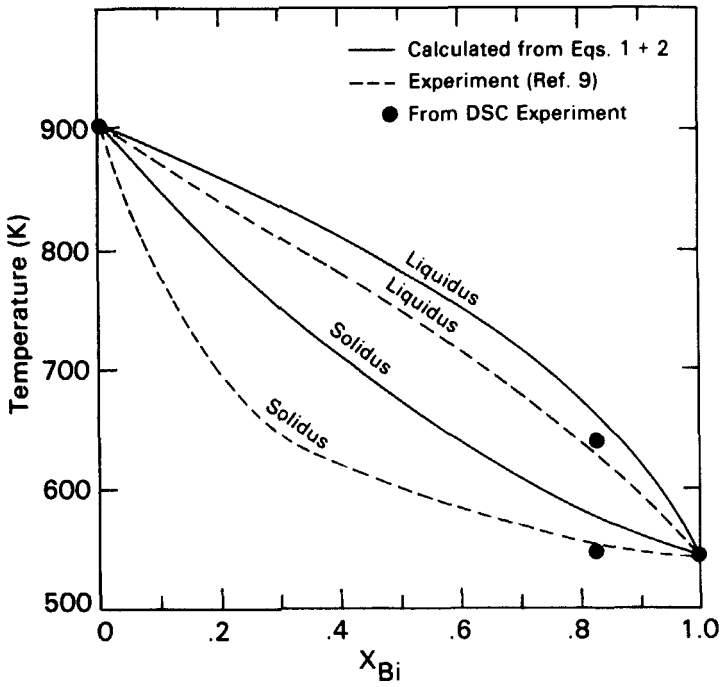

FIGURE 7 Comparison of calculated and experimental phase diagrams for Bi/Sb.

TABLE III

Thermal data for Bi/Sb system

	Melting parameter			
X_{Bi}	T_i(K)	T_f(K)	T_m(K)	L_m(kJ/mol)
1.0 (pure Bi)			544.0[a]	11.05[a]
			544.2[b]	11.00[b]
0.834	~547[a]	~640[a]		11.61[a]
0 (pure Sb)			~900[a,†]	20.12[a]
			903.7[b]	19.87[b]

[a] Present work.

[b] *American Institute of Physics Handbook*, Second Edition, McGraw-Hill, N.Y. (1963).

† This temperature should be taken as nominal since DSC instrument was not calibrated for such a high temperature.

The DSC temperature at onset of melting (T_i) agrees reasonably well with the experimental solidus, but the temperature for completion of melting (T_f) falls between the experimental and calculated liquidus curves. The reason

for the discrepancy is unclear, but may result mainly from the difference in techniques used. The curves of Ref. 9 were determined in cooling, and supercooling did occur, which may account for some of the difference. Such supercooling is clearly observed in the cooling DSC curve of Figure 8. The

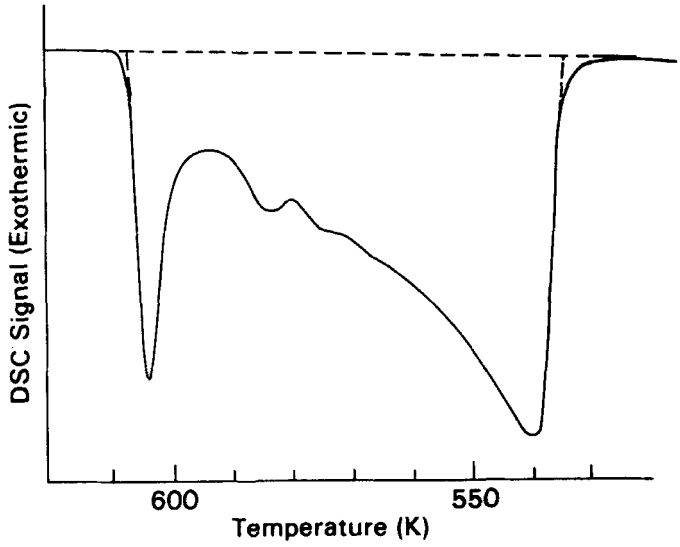

FIGURE 8 DSC cooling curve for Bi/Sb solution ($X_{Bi} = 0.834$). Cooling rate = 20°C/min.

liquidus is supercooled some 30 K (and when first freezing does occur, a "spike" is observed). The solidus is supercooled only about 10 K. Using the program SLHEAT (Table I), we have calculated the ideal solid solution melting curve for Bi/Sb ($X_{Bi} = 0.834$). The predicted line shape is shown in Figure 9. It is clear from a comparison with Figure 6 that the agreement is qualitatively, but not quantitatively correct—further evidence for the non-ideality of the system. Still another indication of non-ideality is apparent from the fact that the latent heat of the binary (Table III) is some 6% less than the value predicted by the straight line of Eq. (16). Since the Bi/Sb system does not approximate an ideal solid solution, we now consider a a third system, 1,12-benzoperylene-coronene.

C 1,12-Benzoperylene/coronene

Melting temperatures and latent heats for "pure" 1,12-benzoperylene and coronene are given in Table IV, along with phase data for a binary mixture of the two components. The experimental DSC curve from which the data for the binary were obtained is given in Figure 10. Two broad transitions are

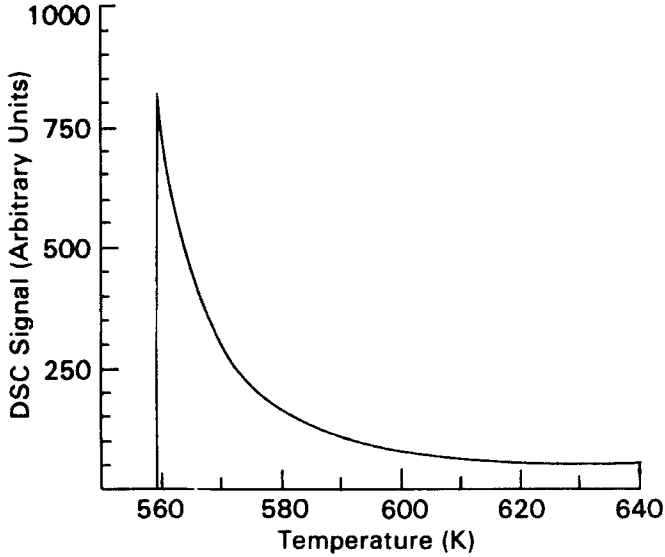

FIGURE 9 Calculated ideal melting curve for Bi/Sb ($X_{Bi} = 0.834$).

TABLE IV

Thermal data for 1,12-Benzoperylene/Coronene System

$X_{1,12\text{-Benzoperylene}}$	Transition type	Transition temp. range (K)	Latent heat (kJ/mole)
1.0 (pure benzoperylene)	melting	553.0[a] 545[b]	17.6[a]
0.687	solid–solid? melting	~566 to ~580[a] ~585 to 621[a]	2.17[a] 14.4[a]
0.0 (pure cornene)	melting	710.5[a] 711[b]	19.2[a]

[a] Present work.
[b] Dictionary of Organic Chemistry, Oxford Press, N.Y. (1965).

visible. Although no solid–solid transitions were observed for either of the pure components, we speculate that the lower temperature peak may correspond to a metastable solid–solid transition or an order-disorder transition.

The broader high temperature peak is undoubtedly associated with melting. Transition temperature ranges and latent heats (determined by planimeter integration of the two peaks) are given in Table IV. The latent heat of the mixture is below that interpolated between the two pure components by means of Eq. (16). However, when the heat for the supposed solid–solid transition is included,[13] the total (16.6 kJ/mol) is in closer agree-

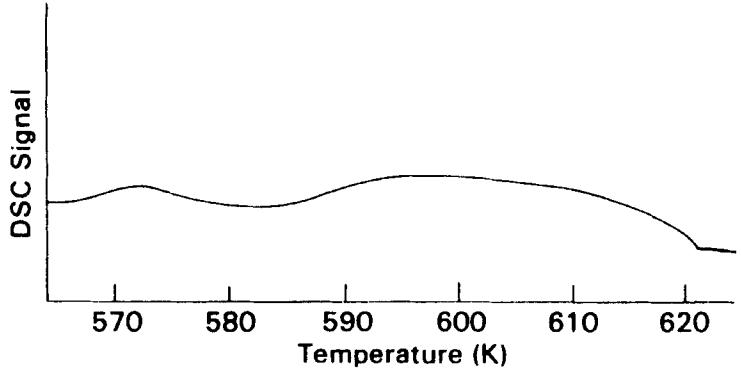

FIGURE 10 DSC melting curve for 1,12-benzoperylene/coronene binary ($X = 0.687$).

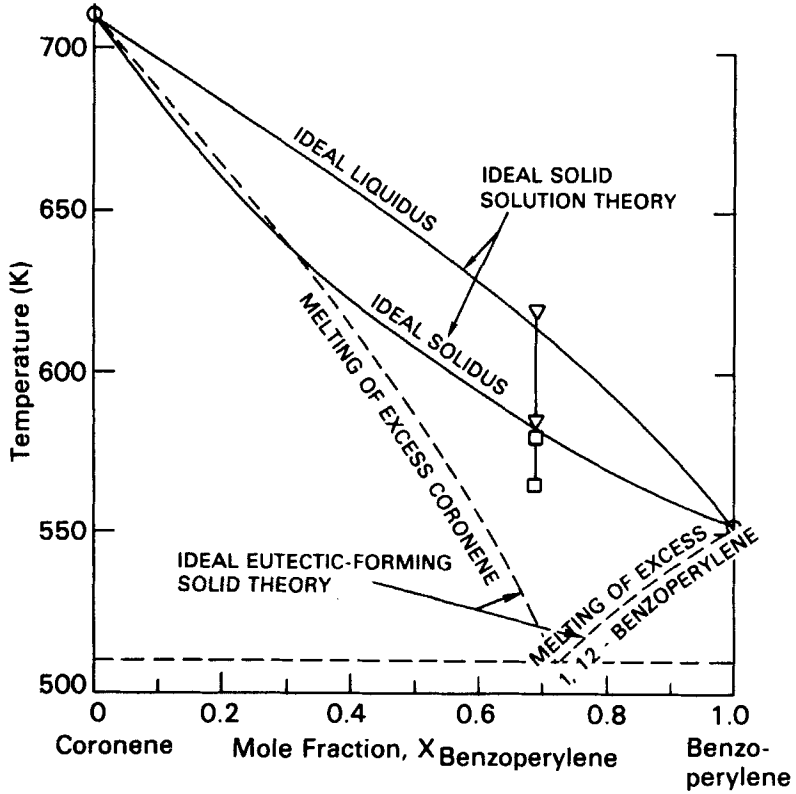

FIGURE 11 Comparison of calculated solid-solution and eutectic-forming system phase diagrams with experiment. The two ▽'s show the observed DSC melting range. The two □'s show the presumed solid-solid transition range.

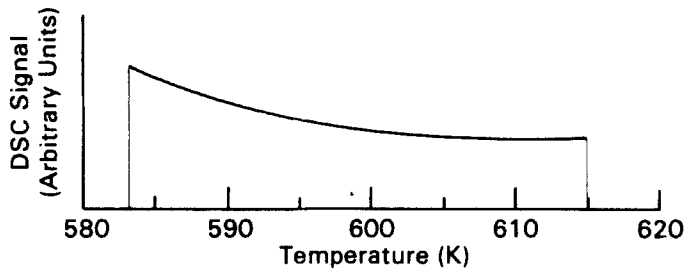

FIGURE 12 Calculated ideal DSC melting curve for 1,12-benzoperylene/coronene system (mole fraction benzoperylene = 0.687).

ment. The remainder of the discrepancy may be due to slight sample degradation in the *in-situ* processing or to difficulty in measuring the area of such a broad peak.

We have calculated phase diagrams for the benzoperylene/coronene system on the basis of two models: ideal solid-solution formation and ideal eutectic formation.[3] The resulting diagrams are plotted in Figure 11. It is evident that the experimental melting range found from Figure 10 agrees well with that calculated from the solid-solution model.

From Eqs. (20–24) we have calculated the ideal solid solution melting curve for the binary (Figure 11). A comparison of Figure 12 with Figure 10 (allowing for instrumental smoothing and broadening), indicates that the agreement is reasonable. It appears that the evidence of both the phase diagram and the melting curve favors an interpretation of benzoperylene/coronene as an ideal solid solution.

CONCLUDING REMARK

Of three systems which possess phase diagrams characteristic of ascending solid solutions, only the two organics appear to approach the ideal case. The melting curve is a useful adjunct to the phase diagram as a test for ideality.

Acknowledgements

The author thanks C. P. Beetz, Jr., J. G. Gay, and J. R. Bradley for useful discussions, and J. C. Price and C. P. Beetz, Jr. for computer programming assistance.

References

1. J. H. Hildebrand and R. L. Scott, *The Solubility of Nonelectrolytes* (Reinhold, New York, 1950).

2. A. Reisman, *Phase Equilibria* (Academic Press, New York, 1970).
3. A. Findlay, *The Phase Rule*, 9th Edition (Dover, New York, 1951).
4. G. W. Smith, *Mol. Cryst. Liq. Cryst.*, **42**, 307 (1977).
5. E. F. Westrum, Jr. and J. P. McCullough, *Physics and Chemistry of the Organic Solid State*, Vol. 1, D. Fox, M. M. Labes, and A. Weissberger, eds. (Interscience, New York, 1963), p. 10.
6. G. W. Castellan, *Physical Chemistry* (Addison-Wesley, Reading, MA, 1964), p. 273.
7. L. H. VanVlack, *Elements of Materials Science and Engineering*, 3rd edition (Addison-Wesley, Reading, MA, 1975), p. 307 ff.
8. The author thanks J. C. Price for performing this modification to the program.
9. *ASM Metals Handbook*, Vol. 8, Eighth Ed., ASM, Metals Park, Ohio (1973). See also M. Hansen, *Constitution of Binary Alloys* (McGraw-Hill, 1958).
10. The sample was prepared by melting Bi in a hermetically sealed DSC Al pan containing Bi + Sb and allowing the Bi to "dissolve" the Sb. Sample uniformity was achieved by cycling the sample through the mixed-phase region several times.
11. Of course, it is conceded that studies at other compositions would be most desirable to test the present model more fully.
12. The mass fractions of the ASM phase diagrams have been converted to mole fractions.
13. G. B. Guthrie and J. P. McCullough, *J. Phys. Chem. Solids*, **18**, 53 (1961).
14. G. B. Thomas, Jr., *Calculus and Analytical Geometry* (Addison-Wesley, Reading, MA, 1960), p. 585 ff.

Appendix I A test for the curvature of the liquidus and solidus curves

Reisman[2] suggests that for low melting latent heats of the pure components, "both the liquidus and solidus are convex with respect to the composition axis" as illustrated schematically in Figure A1. It is the purpose of this note to show that Reisman's statement is not universally correct and to give a more general test of curvature.

For small λ_A and λ_B, the equations for the liquidus and solidus (Eqs. (1) and (2)) take on a simple form:

$$X_A^l = X_A^S = \frac{\lambda_B}{\lambda_B - \lambda_A} \tag{A1}$$

using Eqs. (3) and (4), we find

$$T = \frac{(1 - X_A)L_B + X_A L_A}{X_A S_A + (1 - X_A)S_B} \tag{A2}$$

where $S_A = L_A/T_A$ and $S_B = L_B/T_B$. To determine curvature, we need expressions for dT/dX_A and d^2T/dX_A^2:

$$\frac{dT}{dX_A} = \frac{S_A S_B(T_A - T_B)}{[X_A S_A + (1 - X_A)S_B]^2} \tag{A3}$$

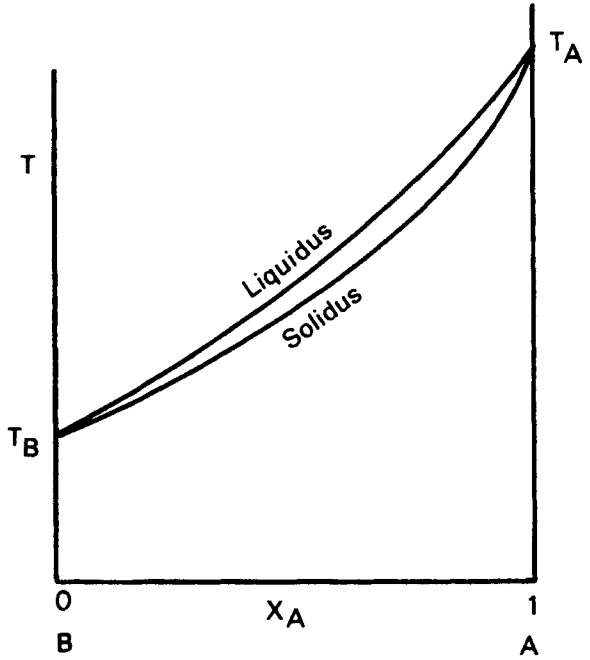

FIGURE A1 Temperature vs. mole fraction A for low L_A and L_B.

$$\frac{d^2T}{dX_A^2} = \frac{-2S_AS_B\left[L_A\left(1-\frac{T_B}{T_A}\right)+L_B\left(1-\frac{T_A}{T_B}\right)\right]}{[X_AS_A+(1-X_A)S_B]^3} \tag{A4}$$

Since all parameters—X_A, S_A, S_B, T_A, and T_B—are positive, it is evident from Eqs. (A3) and (A4) that the sign of slope of the liquidus/solidus is determined by the sign of $(T_A - T_B)$ and the curvature by the sign of d^2T/dX_A^2 and hence of

$$\eta = L_A\left(1-\frac{T_B}{T_A}\right)+L_B\left(1-\frac{T_A}{T_B}\right) \tag{A5}$$

If $\eta < 0$, then $d^2T/dX_A^2 > 0$ and the curvature is upward,[14] in agreement with Reisman's statement. However, if $\eta > 0$, $d^2T/dX_A^2 < 0$ and the curvature is downward, contrary to Reisman's statement. Figures A2 and A3 illustrate these two cases and also show that the criterion of Eq. (A5) holds even in the situation when $X_A^l \neq X_A^s$; i.e. even when λ_A and λ_B are not sufficiently small for Eq. (A1) to be true.

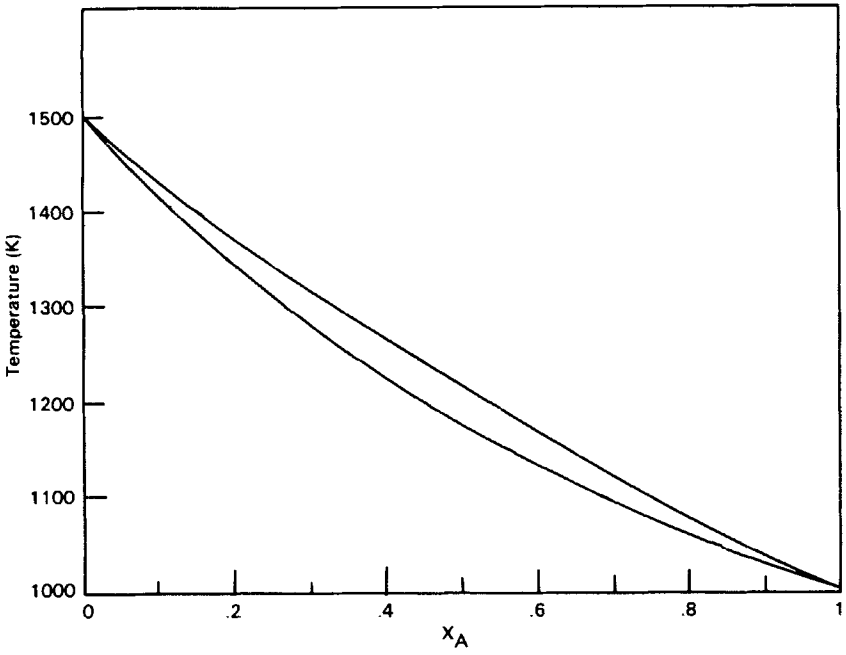

FIGURE A2 Calculated ideal solid-solution phase diagram for $T_A = 1000$ K, $L_A = 8.368$ kJ/mol; $T_B = 1500$ K, $L_B = 8.368$ kJ/mol. For this system $\eta < 0$. Hence $d^2T/dX_A^2 > 0$ and the liquidus and solidus both curve upward.

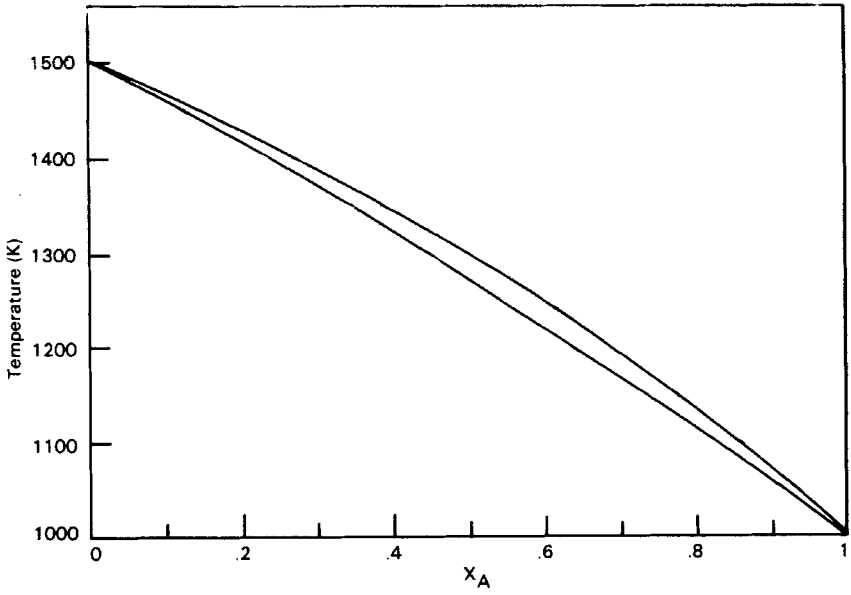

FIGURE A3 Calculated ideal solid-solution phase diagram for $T_A = 1000$ K, $L_A = 4.184$ kJ/mol; $T_B = 1500$ K, $L_B = 8.368$ kJ/mol. For this system $\pi > 0$. Hence $d^2T/dX_A^2 < 0$ and the liquidus and solidus both curve downward.

Appendix II Calculated melting curves for 1,12-benzoperylene/coronene

In this Appendix, for the sake of completeness, we show a number of melting curves calculated (from Eqs. (20–24)) for 1,12-benzoperylene/coronene binary mixtures. In Figure A4 a–f curves, generated by the computer plotting

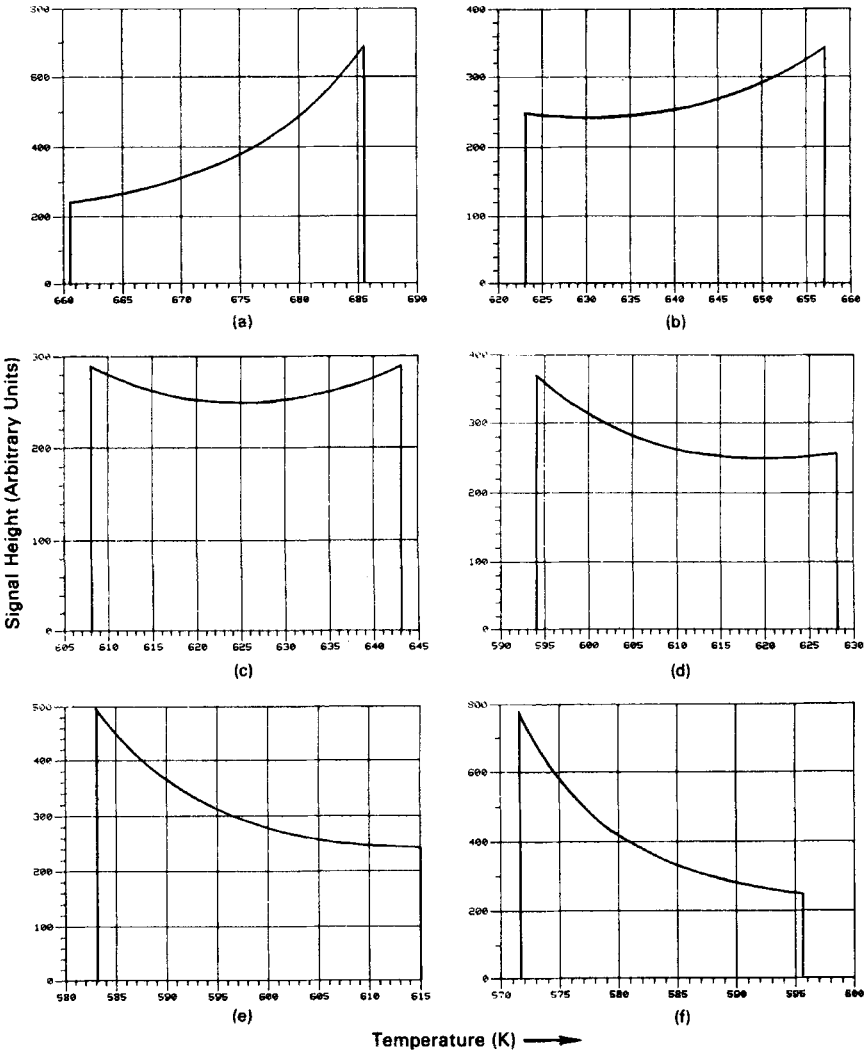

FIGURE A4 Calculated melting curves for 1,12-benzoperylene/coronene with $X = 0.2$ (a), 0.4 (b), 0.5 (c), 0.6 (d), 0.687 (e), and 0.8 (f). Signal heat (ordinate) is plotted versus temperature (K) (abscissa).

routine for $X_{1,12-\text{benzoperylene}} = 0.2, 0.4, 0.5, 0.6, 0.6872$ (the system experimentally studied), and 0.8 are given. The vertical and horizontal scales vary for the curves. It is apparent that further study to test the experimental validity of these curves would be of interest.

To give a better feeling for predicted relative DSC signal strengths, maximum calculated melting curve amplitude is plotted versus X in Fig. A5. It must be emphasized that, because of the lack of instrumental (or other) sources of broadening in the model, the calculated signal height is undoubtedly over-emphasized as $X \to 0$ and $X \to 1$.

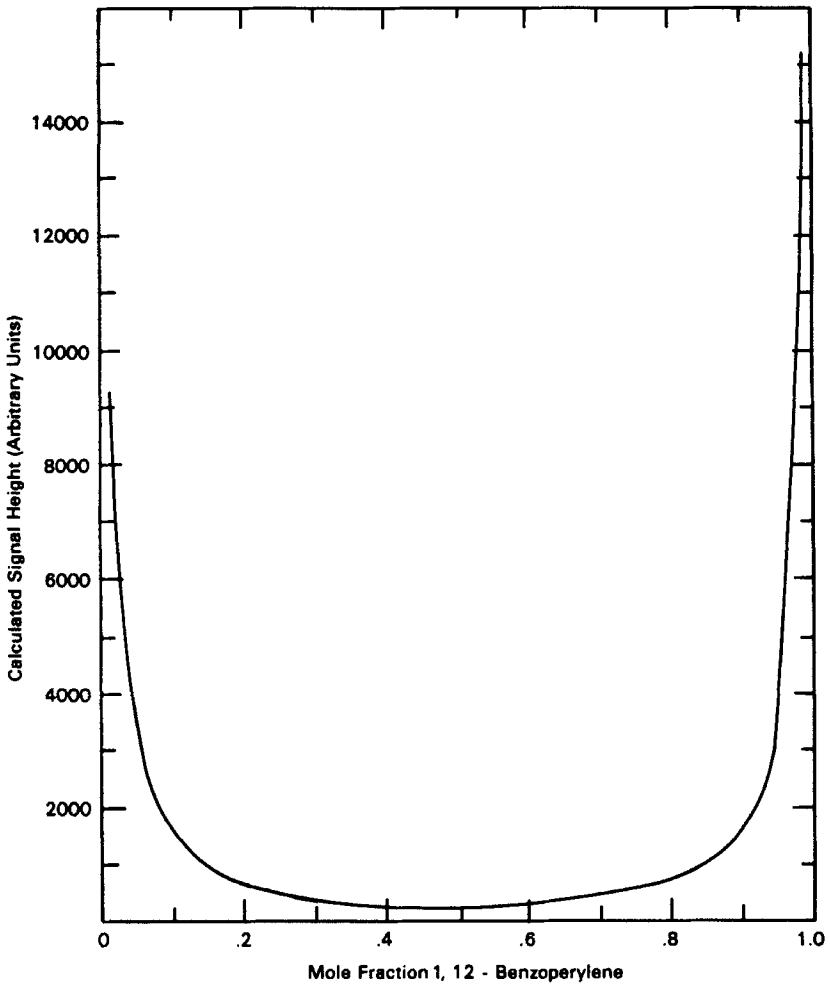

FIGURE A5 Calculated maximum melting curve amplitude vs. X.